Journal of Materials Science and Chemical Engineering, 2024, 12, 14-22
https://www.scirp.org/journal/msce
ISSN Online: 2327-6053
ISSN Print: 2327-6045

A Pioneering Approach to the Synthesis of Silver Nanoparticles

Wasan A. Al-Dulaimi, Zeena M. Al-Azzawi, Emad K. Al-Shakarchi

Physics Department, College of Science, Al-Nahrain University, Baghdad, Iraq
Email: wassan.ali@nahrainuniv.edu.iq, zeena.mowafaq@nahrainuniv.edu.iq, emad.abbas@nahrainuniv.edu.iq

How to cite this paper: Al-Dulaimi, W.A., Al-Azzawi, Z.M. and Al-Shakarchi, E.K. (2024) A Pioneering Approach to the Synthesis of Silver Nanoparticles. *Journal of Materials Science and Chemical Engineering*, **12**, 14-22.
https://doi.org/10.4236/msce.2024.127002

Received: June 10, 2024
Accepted: July 20, 2024
Published: July 23, 2024

Abstract

Our research introduces a groundbreaking chemical reduction method for synthesizing silver nanoparticles, marking a significant advancement in the field. The nanoparticles were meticulously characterized using various techniques, including optical analysis, structural analysis, transmission electron microscopy (TEM), and field-emission scanning electron microscope (FESEM). This thorough process instills confidence in the accuracy of our findings. The results unveiled that the silver nanoparticles had a diameter of less than 20 nm, a finding of great importance. The absorption spectrum decreased in the peak wavelength range (405 - 394 mm) with increasing concentrations of Ag nanoparticles in the range (1 - 5%). The XRD results indicated a cubic crystal structure for silver nanoparticles with the lattice constant (a = 4.0855 Å), and Miller indices were (111), (002), (002), and (113). The simulation on the XRD pattern showed a face center cubic phase with space group Fm-3m, providing valuable insights into the structure of the nanoparticles.

Keywords

Chemical Reduction Method, UV-VIS Absorption Spectrometer, Field-Emission Scanning Electron Microscope (FESEM), Transmission Electron Microscopy (TEM)

1. Introduction

Our research explores the rapid application of nanostructures, mainly silver nanoparticles (AgNPs), in various nanotechnology areas like electronics, catalysis, ceramics, magnetic data storage, and structural components [1]. The unique features of AgNPs make them highly beneficial in biomedical applications, especially in cancer diagnosis and therapy. They can revolutionize antimicrobial agents, drug-delivery formulations, detection and diagnosis platforms, bioma-

terial and medical device coatings, tissue restoration and regeneration materials, complex healthcare condition strategies, and performance-enhanced therapeutic alternatives [2]. The potential of these applications is not just promising but also exciting. In our study, we employed the bottom-up technique, also known as the up-down technique, which involves accumulating atoms to produce nanoparticles. Though more complex, this method is highly efficient and requires high technology. On the other hand, the top-down technique, which is more straightforward, involves the decomposition of bulk material into the nanostructure [3]. This distinction provides valuable knowledge about the different methods of producing nanoparticle powders and their efficiency, and it is a crucial aspect of our research.

Many techniques are used to prepare a silver nanoparticle powder, including a chemical reduction method [1] [4]. Traditionally, a Turkevich procedure extracts any element, such as nanoparticle powder, from a chemical compound [5]. In other words, many chemical and physical processes transfer the bulk material into the nanostructure. However, the reduction method is a powerful technique used to produce nanoparticles by the top-down procedure [4] [6]. The reason for applying this technique is related to its simplicity and reproducibility in producing spherical particles in the range (10 - 30 nm) [5]. The second thing is that it is non-toxic and stabilized by citrate ions. Finally, it has fast nucleation in the synthesis of nanoparticle powders with a narrow size distribution [7]. It was possible to prepare monodisperse gold nanocrystals with a size range (20 - 40 nm) from the chemical solution having (pH = 6.2 - 6.5) [8]. It was applied by increasing the reactivity of the precursor.

There is a new technique for extracting silver nanoparticles (AgNPs) from the Diospyrosmaritima Blume plant. They extract $AgNO_3$ during a reaction time (0.416, 2, 3, 24, 48, and 96 hrs). The phytochemical screening results showed that the leaf extract ofDiospyrosmaritimacontained phenols, flavonoids, saponins, and alkaloids, which may act as a reducing agent of Ag and AgO [9]. On the other hand, AgNPs are very effective in medical applications, for example, as antibacterial, antifungal, antiviral, anti-inflammatory, anti-angiogenic, and anti-cancer agents, and the mechanism of the anti-cancer activity of AgNPs [10].

There is a new technique for preparing silver nanoparticles: the injection method. Through TEM analysis, they conclude a wide range of particle sizes (12 - 20 nm) and their shapes [11]. Usually, the absorption spectrum of Ag nanoparticles is used to determine the particle size. The change in the liquid color of the nanoparticles to transparent orange and then blackish brown is a function of the concentration of nanoparticles. It was found that the absorption peak of silver nanoparticles was at a wavelength of 420 nm related to (50 - 350 nm) [12]. Experimentally, Ag nanoparticle preparation was done using the reduction method. The scientific specification of Ag nanoparticles is characterized by transmission electron microscope (TEM), field emission scanning electron microscope (FESEM), UV-VIS spectrophotometer, and X-ray diffraction. The research aims to compare the nanoparticle production of silver metal with that of standard metal.

2. Experimental Procedure

The reduction method is a simple chemical process used to prepare silver nanoparticles. It is a bottom-up procedure because the chemical reduction tends to produce Ag-atoms, which accumulate to produce nanoparticles. If the reaction rate is too fast, many metal nuclei will suddenly form through the synthesis process, and then the resultant particles are too small [13]. On the other hand, particle agglomerations will occur if the reaction rate is too slow [14]. The chemical reaction used silver nitrate ($AgNO_3$), glucose and polyvinylpyrrolidone (PVP) $(C_6H_9NO)_n$, and sodium hydroxide. The silver nanoparticles were reduced from the silver nitrate in the PVP aqueous solution. The glucose is used as a reducer, and sodium hydroxide is applied to accelerate the reaction. Firstly, the silver nitrate solution was prepared by adding (3.4 g) of $AgNO_3$ into (20 ml) distilled water, making a solution (a). The PVP solution was prepared by dissolving PVP, glucose, and sodium hydroxide in (60 ml) of distilled water, making a solution (b). The last solution is heated to a temperature (60°C) by a magnetic stirrer. After the temperature was fixed for (15 min), the solution (a) was added to (b) as drops. Then, the mixture is stirred for (10 - 15 min). The particles were separated by centrifugation, and the products were washed with distilled water many times to remove the possibility of NO_3 that had not been reacted [15].

3. Results and Discussion

After successive preparations of silver nanoparticles, many analyses and measurements are performed to show the presence of Ag-nanoparticles prepared using a reduction method. These analyses and measurements were used to specify Ag nanoparticles experimentally. The absorption spectrum of Ag nanoparticles was determined using a UV-VIS spectrophotometer for all samples at different concentrations. The absorption spectrum analysis is stated to understand the excitation of electronic states of atoms. It gives more details in the atomic excitation from one level (S^o) to another (Sp), shown in **Figure 1**, for different concentrations of (1 - 5%), respectively. The spectrum depends on the concept of surface Plasmon of Ag nanoparticles produced. The surface Plasmon spectrum (SPS) of Ag nanospheres was mentioned at (400 nm) wavelength for the sample (1%) concentration. At the same time, the surface Plasmon spectrum of the Ag nanostructure was denoted at a wavelength of (397 nm) for the concentration (3%). The concentration (5%) noted that the maximum absorption peak occurred at (394 nm). That means the maximum absorption peak of surface Plasmon absorbance of Ag nanoparticles goes toward a short wavelength as the concentration increases.

Meanwhile, the absorption coefficient decreased as the concentration increased, as mentioned in **Figure 1**. These results are better than those recorded by Singh *et al*. [16]. They recorded the maximum absorption peaks at values

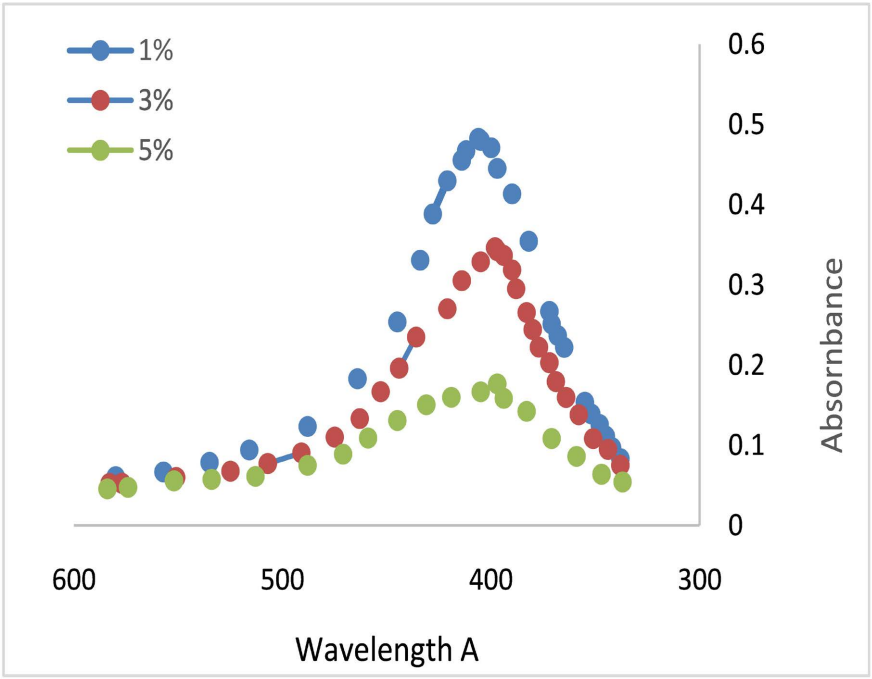

Figure 1. indicates the UV-VIS spectrum for silver nanoparticle solution with different concentrations (1% - 5%).

(466, 438, and 427 nm) for the concentration (0.4, 0.3, and 0.2 M), respectively. That means the results of SPS, as mentioned in **Figure 1**, are better. That is a return to a decrease in the size of nanoparticles. This confirms the ability to obtain a smaller size of the nanoparticle. Theoretically and experimentally, it was found that when size decreases, the SPR peak shifts towards a shorter wavelength side [17].

Transmission electron microscopy (TEM), for different concentrations, is the best technique to distinguish the size and shape of the silver nanostructures shown in **Figure 2**. There is a spherical shape with a particle size in the range (10 - 17 nm). The average value of nanoparticle size is about (14.662 nm). The silver nanoparticles also showed high monodispersed. That is in agreement with the previous studies [17] [18]. The most important thing mentioned in **Figure 2** is the creation of 1D nanostructures like nanowires by assembling nanoparticles in a specific 1D shape.

The results of FESEM are in agreement with TEM results. It showed the appearance of nanoparticles with their morphology distribution on the surface and the homogeneity of grain size in the range (54 - 78 nm) that appeared in **Figure 3**, which agrees with previous studies [19] [20]. The results showed the appearance of silver nanoparticles in different sizes. In addition, the accumulation of silver nanoparticles is increasing silver nanoparticles rather than the size of the nanoparticles, as concluded in TEM results. The agglomeration happened because of the high conductivity of silver metal under the effect of the electron beam of FESEM.

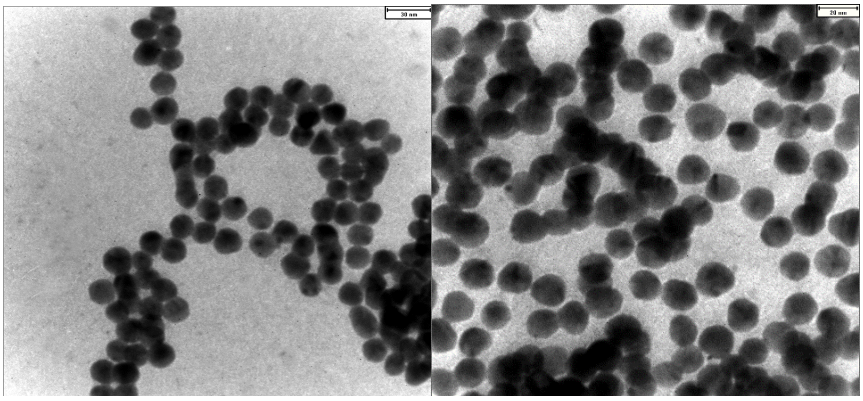

(a) (b)

Figure 2. Shows the TEM results for silver nanoparticles.

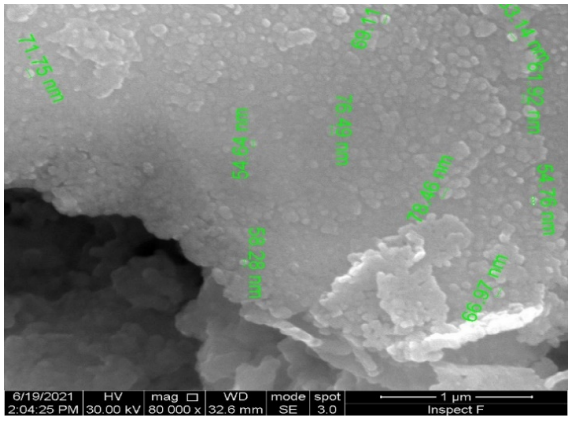

Figure 3. The FESEM results for silver nanoparticles with different positions.

The crystal structure during the XRD pattern, as shown in **Figure 4**, was analyzed using CrysalDiff software to find the structural type and the lattice constants obtained through the simulation. The simulation must be compared with a database (1100136). The simulated data showed a cubic phase with lattice constants (a = 4.0855 Å), and the volume of the unit cell is (68.1923 Å^3). The peak modeling mentioned by the Miller planes labeled (111), (002), (022), and (113) were different from previous studies [1] [21]. The appearance of limited peaks is a sign of a single phase observed, and the sharp diffracted peaks indicate a high degree of crystallinity and smaller grain size. The determination of lattice constants and the crystal phase related to the position of the peaks at a diffracted angle (2θ) and agreement with the database. The high width of peaks is proof of the nanoparticle's appearance. Secondly, the peak intensity (111) is a predominant orientation of a polycrystalline phase produced. Meanwhile, there are other orientations mentioned by (002), (022), and (113) with lower density incomparable with (111). The simulation of the XRD pattern, as mentioned in **Figure 4**, uses Endeavour software to conclude the type of crystal phase. A face-centered cubic was found, as mentioned in **Figure 5**. The theoretical density was about (10.506 g/cm^3). Then, by applying the following equation to find the practical

density

$$\rho_{ex} = \frac{zM}{N_a a^3}$$

Where ($z = 4$) is the number of atom/ unit cell, ($M = 108$) is the atomic weight of Ag, (Na) is Avogadro number, and (a^3 = 68.19 Å^3). Then, experiential density (10.5 g/cm^3) was found was found. The approach between the theoretical and practical density is a function of low vacancy, including in the structure, and producing a highly dense sample. The last is a function of low porosity. Then, apply the following equation to find the probable porosity.

$$P\% = \frac{d_{th} - d_{ex}}{d_{ex}} \times 100$$

It was found that the porosity of about (0.06%) emphasizes the presence of nanoparticles because the presence of nanostructure is related to a decrease in the porosity comparison with the microstructure. On the other hand, the surface area was about (36.7 m^2/g); the suitable equation for calculation is:

$$S = \frac{6}{d_{ex} D}$$

Where (D) is the particle size, it is clear that there is an inverse relationship between the surface area and particle size. This is the second proof of appearing nanoparticles. The recording of high surface area is comparable with a previous study [22] [23].

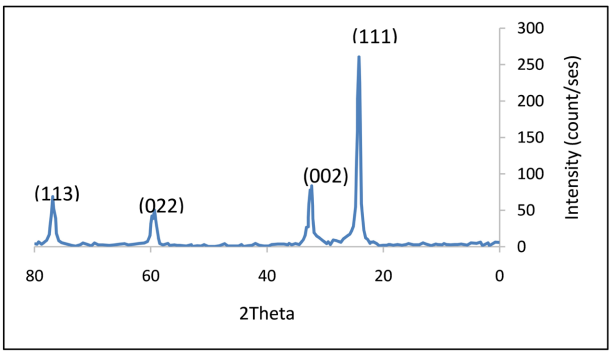

Figure 4. XRD pattern of silver nanoparticle.

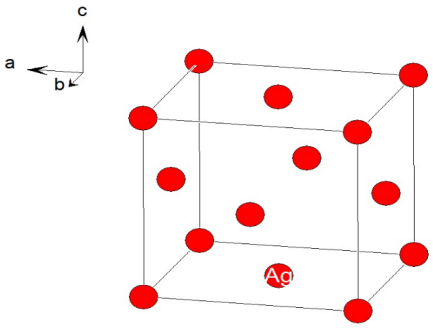

Figure 5. The structural prediction of silver nanoparticle.

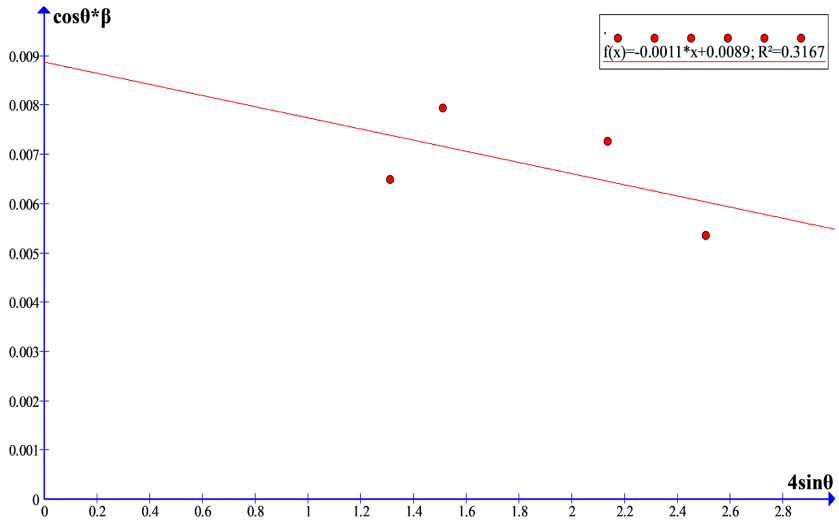

Figure 6. Explains the application of the Williamson-Hall equation.

The XRD analysis is used to determine the crystallite size, which is a sign of the appearance of the nanoparticle. There is a scattering in the points mentioned in **Figure 6** related to a wide range in crystallite size, whereas the straight line is associated with the average crystallite size value. In addition, it is necessary to conclude the elastic strain that might be exhibited within the unit cell during the lattice constants (a, b, c) by applying the Williamson-Hall equation, as mentioned in **Figure 6**. The plotting ($\beta\cos\theta$) on Y-axis versus ($\sin\theta$) on X-axis is producing a straight line equation. The components of this equation are the strain component (4ε) coming from the slope of a straight line and the intercept with the Y-axis related to the crystallite size component ($0.9\lambda/D$). The equation of a straight line is given by:

$$F(x) = 0.0011x + 0.0089$$

The first term is related to elastic strain in the crystal structure, which is a function of the slope of the line. The second term is related to crystallite size, a function of the intercept of a straight line with the Y-axis. The Williamson-Hall method is more accurate than the Debye-Scherer method because the Williamson-Hall method produces a simulated equation for measuring crystallite size and elasticity, as mentioned above. The results showed that the crystallite size is about (15.57 nm) comparable with results obtained by the Scherer formula [24]. It is approaching a particle size discussed by TEM results before. The beneficial thing related to elastic strain (h) is about (0.0002). It is tiny, a function of the minimal variation in a unit cell, and then it relates to the high stability of the cubic phase produced.

4. Conclusion

A chemical reduction method is a simple technique to produce Ag nanoparticles experimentally. It was a perfect technique for producing metallic elements like silver at different concentrations. The nanoparticle size was smaller than (20

nm), which is more favorable than that imported from the external company. Then, it can be used commercially to mass produce any metallic element. The output results are robust in producing nanoparticle powder suitable for application in the medical field through the obtainable results.

Conflicts of Interest

The authors declare no conflicts of interest regarding the publication of this paper.

References

[1] Lai, F., Lin, Z. and Zhang, P. (2018) Preparation and Characterization of Micro/Nano-Silver Powders. *AIP Conference Proceedings*, **1995**, Article 0200101. https://doi.org/10.1063/1.5048741

[2] Burdușel, A.C., Gherasim, O., Grumezescu, A.M., Mogoantă, L., Ficai, A., Andronescu, E. (2018) Biomedical Applications of Silver Nanoparticles: An Up-to-Date Overview. *Nanomaterials*, **8**, Article 681. https://doi.org/10.3390/nano8090681

[3] Xu, L., Wang, Y.Y., Huang, J., Chen, C.Y., Wang, Z.X. and Xie, H. (2020) Silver Nanoparticles: Synthesis, Medical Applications, and Biosafety. *Theranostics*, **10**, 8996-9031. https://doi.org/10.7150/thno.45413

[4] Zhang, H.X., Siegert, U., Liu, R. and Cai, W. (2009) Facile Fabrication of Ultrafine Copper Nanoparticles in Organic Solvent. *Nanoscale Research Letters*, **4**, 705-708. https://doi.org/10.1007/s11671-009-9301-2

[5] Dong, J., Carpinone, P.L., Pyrgiotakis, G., Demokritou, P. and Moudgil, B.M. (2020) Synthesis of Precision Gold Nanoparticles Using Turkevich Method. *KONA Powder and Particle Journal*, **37**, 224-232. https://doi.org/10.14356/kona.2020011

[6] Camacho-Flores, B.A., Martínez-Álvarez, O., *et al*. (2015) Copper: Synthesis Techniques in Nanoscale and Powerful Application as an Antimicrobial Agent. *Journal of Nanomaterials*, **2015**, Article ID: 415238. https://doi.org/10.1155/2015/415238

[7] Zhao, P., Li, N. and Astruc, D. (2013) State of the Art in Gold Nanoparticle Synthesis. *Coordination Chemistry Reviews*, **257**, 638-665. https://doi.org/10.1016/j.ccr.2012.09.002

[8] Ji, X., Song, X., Li, J., Bai, Y., Yang, W. and Peng, X. (2007) Size Control of Gold Nanocrystals in Citrate Reduction: The Third Role of Citrate. *Journal of the American Chemical Society*, **129**, 13939-13948. https://doi.org/10.1021/ja074447k

[9] Agustina, T.E., Handayani, W. and Imawan, C. (2020) The UV-VIS Spectrum Analysis from Silver Nanoparticles Synthesized Using *Diospyros maritima* Blume. Leaves Extract. *Advances in Biological Sciences Research*, **14**, 411-419.

[10] Zhang, X.F., Liu, Z.G. W.S., *et al*. (2016) Silver Nanoparticles: Synthesis, Characterization, Properties, Applications and Therapeutic Approaches. *International Journal of Molecular Sciences*, **17**, Article 1534. https://doi.org/10.3390/ijms17091534

[11] Noritomi, H., Miyagawa, S., Igari, N., Saito, H. and Kato, S. (2013) Application of Reverse Micelles of Alkyl Glucosides to Synthesis of Silver Nanoparticles. *Advances in Nanoparticles*, **2**, 344-349. https://doi.org/10.4236/anp.2013.24047

[12] Mohammed Ali, I.A. Ahmed, A.B. and Al-Ahmed, H.I. (2023) Green Synthesis, and Characterization of Silver Nanoparticles for Reducing the Damage to Sperm Parameters in Diabetic Compared to Metformin. *Scientific Reports*, **13**, Article No. 2256. https://doi.org/10.1038/s41598-023-29412-3

[13] Badi, S.J., Al-Shakarchi, E.K. and Ahmed, S.J. (2020) The Effect of Gold Salt Concentration in the Production of Gold Nanosphere, *Journal of Applied Mathematics and Physics*, **8**, 1487-1495. https://doi.org/10.4236/jamp.2020.88114

[14] Sertbakan, T.R., Al-Shakarchi, E.K. and Mala, S.S. (2022) The Preparation of Nano Silver by Chemical Reduction Method. *Journal of Modern Physics*, **13**, 81-88. https://doi.org/10.4236/jmp.2022.131006

[15] Wang, H., Qiao, X., Chen, J. and Ding, S. (2005) Preparation of Silver Nanoparticles by Chemical Reduction Method. *Colloids and Surfaces A*: *Physicochemical and Engineering Aspects*, **256**, 111-115. https://doi.org/10.1016/j.colsurfa.2004.12.058

[16] Singh, S., Bharti, A. and Meena, V.K. (2015) Green Synthesis of Multi-Shaped Silver Nanoparticles: Optical, Morphological and Antibacterial Properties. *Journal of Materials Science: Materials in Electronics*, **26**, 3638-3648. https://doi.org/10.1007/s10854-015-2881-y

[17] Das, R., Nath, S.S. Chakdar, D., Gope, G. and Bhattacharjee, R. (2010) Synthesis of Silver Nanoparticles and Their Optical Properties. *Journal of Experimental Nanoscience*, **5**, 357-362. https://doi.org/10.1080/17458080903583915

[18] Khanal, L.N., Sharma, K.R., Paudyal, H., Parajuli, K., Dahal, B., Ganga, G.C., Pokharel, Y.R. and Kalauni, S.K. (2022) Green Synthesis of Silver Nanoparticles from Root Extracts of *Rubusell ipticus* Sm. and Comparison of Antioxidant and Antibacterial Activity. *Journal of Nanomaterials*, **2022**, Article ID: 1832587. https://doi.org/10.1155/2022/1832587

[19] Nayak, B.K., Chitra, N. and Nanda, A. (2014) Efficacy of Biosynthesized AgNPs from Alternaria Chlamydospora Isolated from Indoor Air of Vegetable Market. *International Journal of PharmTech Research*, **6**, 1309-1314.

[20] Verma, S.K., Jha, E., Sahoo, B., Panda, P.K., Thirumurugan, A., Parashar, S.K.S. and Suar, M. (2017) Mechanistic Insight into the Rapid One-Step Facilebio Fabrication of Antibacterial Silver Nanoparticles from Bacterial Release and Their Biogenicity and Concentration-Dependent *in Vitro* Cytotoxicity Tocolon Cells. *RSC Advances*, **7**, 40034-40045. https://doi.org/10.1039/C7RA05943D

[21] Mehta, B.K., Chhajlani, M. and Shrivastava, B.D. (2017) Green Synthesis of Silver Nanoparticles and Their Characterization by XRD. *Journal of Physics*: *Conference Series*, **836**, Article 012050. https://doi.org/10.1088/1742-6596/836/1/012050

[22] Zhou, M.R., Wei, Z.W., *et al*. (2009) Particle Size and Pore Structure Characterization of Silver Nanoparticles Prepared by Confined Arc Plasma. *Journal of Nanomaterials*, **2009**, Article ID: 968058. https://doi.org/10.1155/2009/968058

[23] Ahmad, T., Nazim, V.A., *et al*. (2020) Biosynthesis, Characterization and Photo-Catalytic Degradation of Methylene Blue Using Silver Nanoparticles. *Materials Today*: *Proceedings*, **29**, 1039-1043. https://doi.org/10.1016/j.matpr.2020.04.707

[24] Kanwal, Z., Raza, M.A., Riaz, S., Manzoor, S., Tayyeb, A., Sajid, I. and Naseem, S. (2019) Synthesis and Characterization of Silver Nanoparticle-Decorated Cobalt Nanocomposites (Co@AgNPs) and Their Density-Dependent Antibacterial Activity. *Royal Society Open Science*, **6**, 1821351-18213515. https://doi.org/10.1098/rsos.182135